# Mimicking Photosynthesis to Make Functional Nanostructures and Nanodevices

J. A. Shelnutt[*,**], Z. Wang[*,**], Y. Song[*], C. J. Medforth[*] and E. Pereira[***]

[*]Sandia National Laboratories, Albuquerque, NM, USA, jasheln@sandia.gov
[**]University of Georgia, Athens, GA, USA, jasheln@unm.edu
[***]Universidade do Porto, Porto, Portugal, efpereir@fc.up.pt

## ABSTRACT

The processes and functional constituents of biological photosynthetic systems can be mimicked to produce a variety of functional nanostructures and nanodevices. The photosynthetic nanostructures produced are analogs of the naturally occurring photosynthetic systems and are composed of biomimetic compounds (*e.g.*, porphyrins). For example, photocatalytic nanotubes can be made by ionic self-assembly of two oppositely charged porphyrins tectons [1]. These nanotubes mimic the light-harvesting and photosynthetic functions of biological systems like the chlorosomal rods and reaction centers of green sulfur bacteria. In addition, metal-composite nanodevices can be made by using the photocatalytic activity of the nanotubes to reduce aqueous metal salts to metal atoms, which are subsequently deposited onto tube surfaces [2]. In another approach, spatial localization of photocatalytic porphyrins within templating surfactant assemblies leads to controlled growth of novel dendritic metal nanostructures [3].

***Keywords***: porphyrin, photocatalyst, nanotube, metal, nanodevice

## 1 PORPHYRIN NANOTUBES

Porphyrins and other tetrapyrroles such as chlorophylls play important functional roles in biological nanostructures and proteins of photosynthetic systems. The chlorophyll molecules are sometimes self-organized into nanoscale superstructures that perform essential light-harvesting and energy- and electron-transfer functions. An example of the biological nanostructures formed by chlorophyll is the light-harvesting chlorosomal rods of the photosynthetic pseudo-organelles of green-sulfur bacteria, called chlorosomes. The chlorosomal rods are composed entirely of aggregated bacteriochlorophyll molecules as illustrated in Figure 1. Because of their desirable functional properties, porphyrins are attractive building blocks for a wide variety of functional synthetic nanostructures.

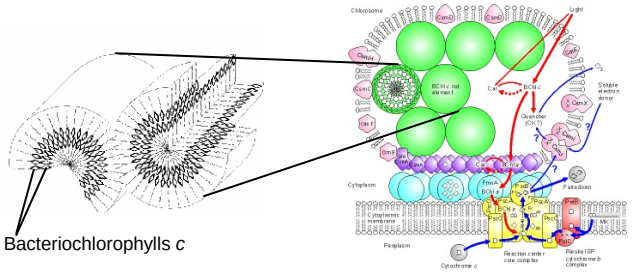


**Figure 1.** A chlorosome on the bacterial membrane contains the chlorosomal rods that harvest light.

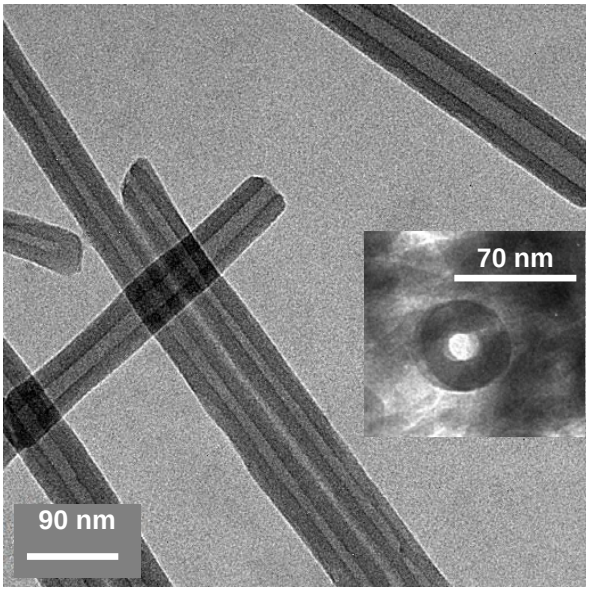


**Figure 2.** Transmission electron microscopy image of the porphyrin nanotubes. Inset: A tube trapped in a vertical orientation by a thick mat of tubes.

Recently, we discovered the first porphyrin nanostructures that possess well-defined morphologies suitable for technological applications [1,2]. An example is the porphyrin nanotubes shown in Figure 2 [1]. These sturdy nanostructures are suitable for incorporation into nanodevices for solar water splitting and other applications. The porphyrin nanostructures are biomimetic since the porphyrins are related to the chlorophyll molecules contained in systems found in nature that carry out light harvesting, charge separation, and energy conversion. Specifically, the porphyrin nanotubes shown in Figure 2 appear to mimic the light-harvesting and reaction-center functions of chlorosomes (Figure 1), and they possess other useful properties.

Our porphyrin nanotubes are prepared by ionic self-assembly of two oppositely charged porphyrins in aqueous solution and are composed entirely of porphyrins such as those shown in Figure 3. The nanotubes are just one member of a new class of porphyrin-based nanostructures that we are developing. We have found that the molecular building blocks (tectons) can be altered to produce a range

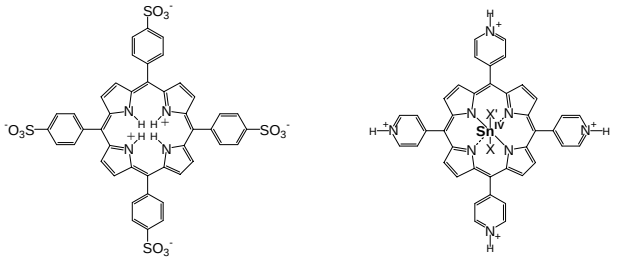


$[H_4TPPS_4]^{2-}$ $[Sn(X)(X')TPyP]^{4+/5+}$

**Figure 3.** Porphyrins used in making the porphyrin nanotubes shown in Figure 2. Sn(IV) will have ligands (X, X' = Cl, OH, $H_2O$) bound above and below the porphyrin plane. At pH 2 where the tubes are assembled, X = OH and X' = $H_2O$ (net charge +5) or X = X' = OH (charge +4).

of nanostructures with different structural and functional properties. The porphyrin nanotubes in Figure 2 are hollow structures with uniform diameter and shape. The strong electrostatic forces between the porphyrin tectons (in addition to the van der Waals, hydrogen-bonding, axial coordination, and other weak intermolecular interactions that typically contribute to the stability of porphyrin aggregates) enhance the structural stability of these new nanostructures.

It has long been known that synthetic porphyrins under certain conditions form aggregates with interesting optical and electronic properties, and these aggregates have sometimes been found in the form of useful nanostructures including fibers, nanorods, or thin stripes on surfaces. However, the aggregates are more typically found as less useful forms such as nanoparticles, sheets, or fractal objects. The nanotubes, nanofibers, and structurally more complex nanostructures recently synthesized by our group satisfy the need for well-defined and robust porphyrin nanostructures that will be useful in many applications, including electronics, photonics, light-energy conversion, and catalysis. In particular, the porphyrin nanotubes and related porphyrin nanostructures possess shapes and functional properties that make them particularly useful for the construction of electronic and photonic nanodevices.

## 1.1 Synthesis of Porphyrin Nanotubes

The self-assembled porphyrin nanotubes are composed of two porphyrin molecules having opposite charges. The porphyrin nanotubes shown in Figure 2 are formed by mixing aqueous solutions of the two porphyrins shown in Figure 3. Typically, 9 mL of $H_4TPPS_4^{2-}$ solution (10.5 μM $H_4TPPS_4^{2-}$, 0.02 M HCl) was mixed with 9 mL of Sn(IV) tetrakis(4-pyridyl)porphyrin ($SnTPyP^{2+}$) dichloride in water (3.5 μM $SnTPyP^{2+}$), and the mixture was left undisturbed in the dark at room temperature for 72 h. Although the individual porphyrins by themselves exhibit negligible aggregation under these conditions (pH 2), the mixture of porphyrins immediately forms colloidal aggregates and, over time, provides a high yield (approximately 90%) of nanotubes. The remaining 10% of the porphyrin material is mostly rod-like with dimensions similar to those of the tubes, and thus appears to be collapsed tubes.

## 1.2 Structure of the Porphyrin Nanotubes

Transmission electron microscope (TEM) images of the porphyrin nanotubes are shown in Figure 2. They reveal that the nanotubes are micrometers in length and have diameters in the range of 50-70 nm with approximately 20-nm thick walls. Images of the nanotubes caught in vertical orientations (*e.g.*, see Inset of Figure 2) confirm a hollow tubular structure with open ends. Fringes with 1.7-1.8-nm spacing are seen both in end-on views and at the edges of the nanotubes in TEM images. The fringes probably originate from the heavy tin and sulfur atoms in the porphyrin stacks. The fringes seen in the TEM images, combined with the optical spectral results discussed below, are consistent with a structure composed of stacks of offset *J*-aggregated porphyrins (individual porphyrins are approximately 2 x 2 x 0.5 nm) likely in the form of cylindrical lamellar sheets. The lamellar structure could be similar to an architecture proposed for the stacking of bacteriochlorophyll molecules in the chlorosomal rods. X-ray diffraction studies (not shown) exhibit peaks in the low- and high-angle regions with line widths suggesting moderate crystallinity.

## 1.3 Composition of the Porphyrin Nanotubes

The composition of the nanotubes was determined by UV-visible absorption spectroscopy and energy dispersive X-ray (EDX) spectroscopy. The filtered nanotubes were dissolved at pH 12 and the ratio of the porphyrins was determined by spectral simulation using extinction coefficients for $H_2TPPS_4^{4-}$ ($\varepsilon_{552}$ = 5500 $mol^{-1}dm^3cm^{-1}$) and $Sn(OH)_2TPyP$ ($\varepsilon_{552}$ = 20200 $mol^{-1}dm^3cm^{-1}$), giving an approximate molar ratio of 2.4 $H_2TPPS_4^{4-}$ per $Sn(OH)_2TPyP$. EDX measurements of the S:Sn atomic ratio of the porphyrin tubes on the TEM grids also indicate a molar ratio of between 2.0 and 2.5. The observed ratio of the two porphyrins in the tubes (2.0-2.5) is related to the charges of the porphyrin species present at pH 2 (see Figure 3). As shown by acid-base titrations monitored by UV-visible spectroscopy, the porphyrin species present at pH 2 are $H_4TPPS_4^{2-}$ and a mixture of $Sn(OH)_2TPyP^{4+}$ and $Sn(OH)(H_2O)TPyP^{5}$, giving a ratio of charges of 2.0 or 2.5.

## 1.4 Properties of the Porphyrin Nanotubes

Porphyrin nanotubes have desirable electronic and optical properties making them suitable for incorporation into electronic and photonic devices. One of the interesting optical properties is the ability of the tubes to resonantly scatter light at the wavelength of the *J* band of the aggregated porphyrins forming the tube walls (particularly the 496-nm band; see Figure 4) [1]. The *J*-aggregate bands

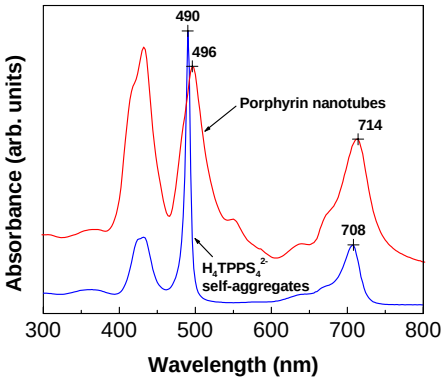


**Figure 4.** UV-visible absorption spectrum (red) of a colloidal suspension of the porphyrin nanotubes and a spectrum of a suspension of the $H_4TPPS_4^{2-}$ self-aggregates formed in 0.3 M HCl (blue) for comparison. The *J*-aggregate bands are near 496 and 714 nm.

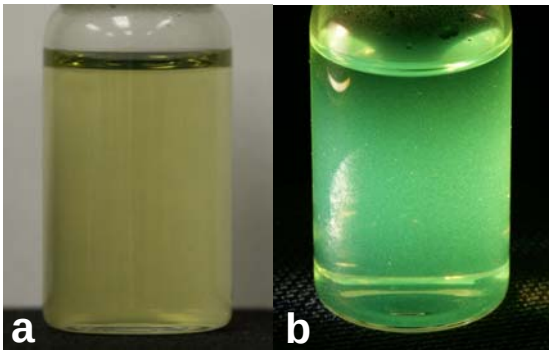


**Figure 5.** Photographs showing a colloidal suspension of porphyrin nanotubes in transmitted white light (a) and the same suspension when viewed perpendicular to a beam of incandescent white light (b). The bright green colour observed in (b) is due to the intense resonance light scattering at the 496-nm *J*-aggregate absorption band.

result from the slipped or off-set stacking of the porphyrins, for which the strong coupling of transition dipoles of several adjacent molecules leads to intense light scattering from the interacting molecules.

The effect of the intense scattering is shown in the comparison of the photographs for weak transmitted light (Figure 5a) and for intense incandescent light directed at right angles to the observer (Figure 5b) for the suspension of the porphyrin nanotubes; the latter shows the intense green color of the resonance scattered light.

Another potentially useful property of the nanotubes is their ability to respond mechanically to light illumination. Even though they are stable for months when stored in the dark, irradiation of a suspension of the tubes for just five minutes using incandescent light from a projector lamp (800 nmol-$cm^{-2}$-$s^{-1}$) results in TEM images showing rod-like structures instead of tubes [1]. This response to light is reversible, as the tubes reform (self-heal) when left in the dark. The tubes have other interesting photochemical properties, including acting as photocatalysts for the reduction of metal complexes in aqueous solution or for the reduction of water to hydrogen (see below).

## 1.5 Control of Nanotube Structure

By altering the molecular structure of the porphyrin tectons, the dimensions of the nanotubes can be controlled. For example, nanotubes made with Sn tetra(3-pyridyl)-porphyrin instead of Sn tetra(4-pyridyl)porphyrin have significantly smaller average diameters (35 nm instead of 60 nm) [1]. Switching to the 3-pyridiyl porphyrin subtly repositions the charge centers and the associated H-bond donor atoms on the pyridinium rings, apparently changing the inter-porphyrin interactions sufficiently to alter the diameter while still allowing the tubes to form. Nanotubes are not produced by the 2-pyridyl porphyrin. Nanotubes are also obtained when $Sn^{4+}$ is replaced with other six-coordinate metal ions (*e.g.*, $Fe^{3+}$, $Co^{3+}$, $TiO^{2+}$, $VO^{2+}$), but tubes have not been observed for four-coordinate metals (*e.g.*, $Cu^{2+}$) or the metal free porphyrin. A high degree of control over the structure of the tubes may be realized by modifying the tectons, including variation of the peripheral substituents of the porphyrin, the metal contained in the porphyrin core, and the nature of the axial ligands. Variation of the metal in particular will also alter the functional properties of the tubes.

# 2 PHOTOCATALYTIC NANOTUBES

Sn porphyrins are known to be good photocatalysts in homogeneous solutions, so we investigated whether the Sn porphyrins in the nanotubes would make the tubes themselves photocatalytic. To demonstrate photocatalytic activity of the tubes we examined the reduction of aqueous metal complexes of Au(I) and Pt(II) [2]. The photosynthetic properties of the nanotubes containing Sn porphyrins shown in Figure 2 have been used to synthesize functional nanotube-metal composite systems, which, in turn, may lead to solar nanodevices that mimic photosynthesis to produce hydrogen fuel by splitting water.

## 2.1 Gold Deposition on Porphyrin Nanotubes

When nanotubes are used to photoreduce the positively charged Au(I)-thiourea complex, the metal is deposited exclusively within the hollow interior of the nanotubes, forming a continuous polycrystalline gold nanowire that is of the same diameter as the tube core (Figure 6a). For those tubes that contain nanowires, only continuous gold wires are found, *i.e.*, multiple short segments are not observed in the same nanotube. In addition, the nanowires are typically terminated at one end of the nanotube with a gold ball of larger diameter than the tube. When the porphyrin nanotubes are dissolved by raising the pH, the gold wire and ball remain intact as shown in Figure 6b. In contrast with the thiourea complex, reduction of the *negatively* charged Au(I) thiosulfate complex produces gold particles

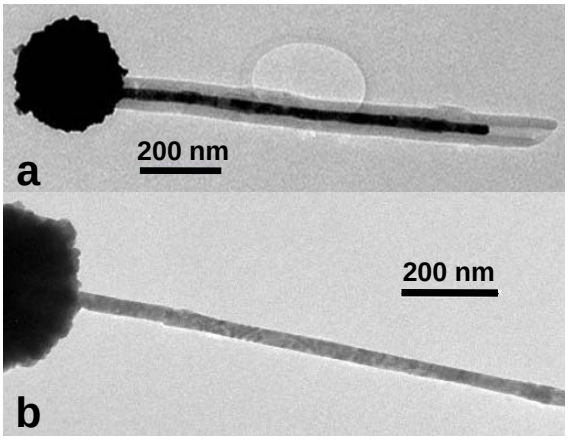


**Figure 6.** TEM images of (a) a gilded nanotube obtained using the Au(I) thiourea complex, and (b) a gold wire obtained after the porphyrin tube has been dissolved away at pH 10 by adding 0.05 M NaOH. The latter demonstrates the structural integrity of the free standing nanowires.

mainly on the outer surfaces of the tubes. Differences in electrostatic and other surface interactions with the complex may determine where metal is deposited. Directional electron/energy transport in the walls might also play a role.

## 2.2 Growth of Platinum Dendrites

Photocatalytic seeding and autocatalytic reduction of platinum and palladium salts leads to remarkable dendritic metal nanomaterials [3]. In micellar solutions, spherical metal nanodendrites are obtained. With liposomes as the template, dendritic platinum sheets in the form of thin circular disks or foam-like Pt nanomaterials (Figure 7) are obtained. Exquisite synthetic control over the morphology of these nanoscale dendrites, sheets, and nanostructured foams is realized by using photocatalytic tin porphyrins. Illumination conveniently and effectively produces a large initial population of catalytic growth centers in the surfactant assemblies. The initial concentration of these seed nanoparticles determines the average size and uniformity of the platinum dendrites, which grow by templating on the surfactant assemblies.

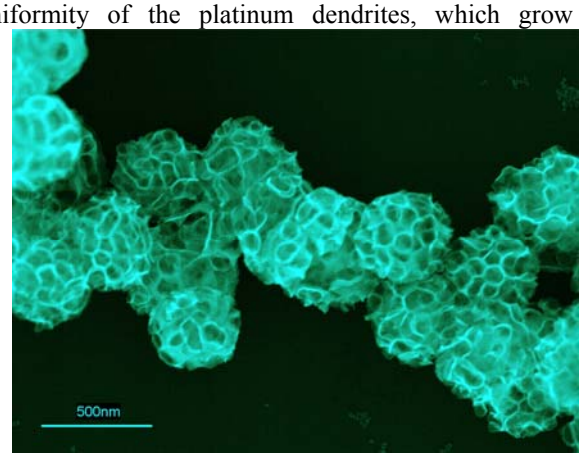


**Figure 7.** SEM image of platinum foam-like nanoballs templated on DSPC/cholesterol liposomes.

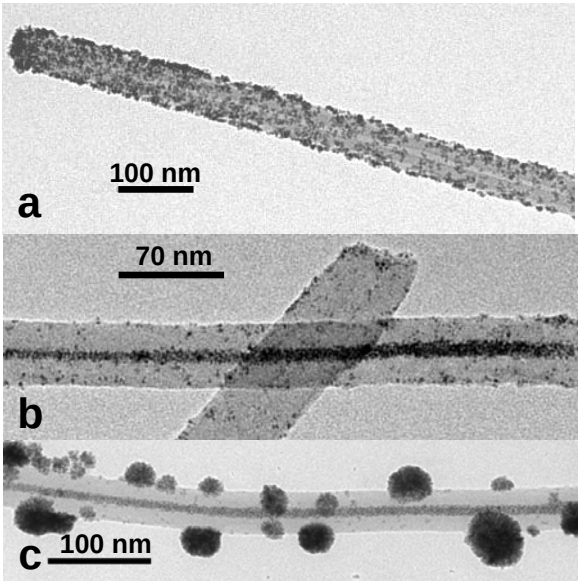


**Figure 8.** TEM images of (a) a platinized porphyrin nanotube with Pt nanoparticles distributed mainly on the outside surface, (b) a long Pt dendrite in the core of the tube obtained at a higher Pt concentration, and (c) a long dendrite in the core and Pt dendrites on the outer surface.

## 2.3 Platinum Deposition on Nanotubes

Figure 8 shows TEM images of some of the nanodevices that can be fabricated by growing Pt particles and dendrites on the porphyrin nanotubes. Figure 8b,c show tubes with dendritic Pt nanowires in the tube cores.

## 3 ACKNOWLEDGEMENTS

This work was partially supported by the Division of Materials Sciences and Engineering, Office of Basic Energy Sciences, U.S. Department of Energy, and by the Division of Chemical Sciences, Geosciences and Biosciences, Office of Basic Energy Sciences, U.S. Department of Energy (DE-FG02-02ER15369). Sandia is a multiprogram laboratory operated by Sandia Corporation, a Lockheed Martin Company, for the United States Department of Energy's National Nuclear Security Administration under Contract DE-AC04-94AL85000.

## REFERENCES

[1] Wang, Z.; Medforth, C. J.; Shelnutt, J. A., *J. Am. Chem. Soc.* **2004**, *126*, 15954-15955.

[2] Wang, Z.; Medforth, C. J.; Shelnutt, J. A., *J. Am. Chem. Soc.* **2004**, *126*, 16720-16721.

[3] Song, Y.; Yang, Y.; Medforth, C. J.; Pereira, E.; Singh, A. K.; Xu, H.; Jiang, Y.; Brinker, C. J.; van Swol, F.; Shelnutt, J. A., *J. Am. Chem. Soc.* **2004**, *126*, 625-635